Society For Biomaterials

Citrate-based biphasic scaffolds for the repair of large segmental bone defects

Ying Guo,[1,2*] Richard T. Tran,[3*] Denghui Xie,[1,2*] Yuchen Wang,[1,2*] Dianna Y. Nguyen,[3] Ethan Gerhard,[3] Jinshan Guo,[3] Jiajun Tang,[1,2] Zhongming Zhang,[1,2] Xiaochun Bai,[1,2] Jian Yang[3]

[1]Department of Orthopedic, Academy of Orthopedics, Guangdong Province, The Third Affiliated Hospital, Southern Medical University, Guangzhou 510280, China
[2]Department of Cell Biology, School of Basic Medical Science, Southern Medical University, Guangzhou 510515, China
[3]Department of Biomedical Engineering, Materials Research Institute, The Huck Institutes of The Life Sciences, The Pennsylvania State University, University Park, Pennsylvania 16802

Received 15 March 2014; revised 5 May 2014; accepted 13 May 2014
Published online 28 May 2014 in Wiley Online Library (wileyonlinelibrary.com). DOI: 10.1002/jbm.a.35228

Abstract: Attempts to replicate native tissue architecture have led to the design of biomimetic scaffolds focused on improving functionality. In this study, biomimetic citrate-based poly (octanediol citrate)-click-hydroxyapatite (POC-Click-HA) scaffolds were developed to simultaneously replicate the compositional and architectural properties of native bone tissue while providing immediate structural support for large segmental defects following implantation. Biphasic scaffolds were fabricated with 70% internal phase porosity and various external phase porosities (between 5 and 50%) to mimic the bimodal distribution of cancellous and cortical bone, respectively. Biphasic POC-Click-HA scaffolds displayed compressive strengths up to 37.45 ± 3.83 MPa, which could be controlled through the external phase porosity. The biphasic scaffolds were also evaluated *in vivo* for the repair of 10-mm long segmental radial defects in rabbits and compared to scaffolds of uniform porosity as well as autologous bone grafts after 5, 10, and 15 weeks of implantation. The results showed that all POC-Click-HA scaffolds exhibited good biocompatibility and extensive osteointegration with host bone tissue. Biphasic scaffolds significantly enhanced new bone formation with higher bone densities in the initial stages after implantation. Biomechanical and histomorphometric analysis supported a similar outcome with biphasic scaffolds providing increased compression strength, interfacial bone ingrowth, and periosteal remodeling in early time points, but were comparable to all experimental groups after 15 weeks. These results confirm the ability of biphasic scaffold architectures to restore bone tissue and physiological functions in the early stages of recovery, and the potential of citrate-based biomaterials in orthopedic applications. J Biomed Mater Res Part A: 103A: 772–781, 2015.

Key Words: biomimetic, biphasic scaffold, biodegradable composite, citrate, elastomer

How to cite this article: Guo Y, Tran RT, Xie D, Wang Y, Nguyen DY, Gerhard E, Guo J, Tang J, Zhang Z, Bai X, Yang J. 2015. Citrate-based biphasic scaffolds for the repair of large segmental bone defects. J Biomed Mater Res Part A 2015:103A:772–781.

INTRODUCTION

Current challenges in the management of large segmental bone defects have driven research in the direction of creating biologically inspired substitutes to replicate the anisotropy, nonlinearity, and local mechanical properties of native bone tissue.[1–3] Bone is a relatively rigid and lightweight organ optimized to withstand external loads through its unique tissue architecture, which is a bimodal distribution of highly porous cancellous bone surrounded by a dense layer of cortical bone.[4,5] The elucidation of this natural structure has provided insights into the design of biomimetic alternatives focused on tissue functionality.[3] For example, various multiphasic and gradient porosity scaffold design strategies have been introduced to mimic the stratified native architecture of bone and provide improved mechanical and biological properties over conventional scaffolds of uniform porosity.[4,6,7] Thus, by simultaneously replicating the respective porosities of dense cortical bone and open network of cancellous bone within a single construct, novel tissue engineered scaffolds can be produced to not only provide long-term regenerative capabilities but also immediate structural and load bearing support.[3]

In addition to recreating the native tissue architectures, selecting the appropriate biomaterial for scaffold fabrication

*These authors contributed equally to this work.
Correspondence to: Z. Zhang; e-mail: 13002006619@163.com or X. Bai; e-mail: baixc15@smu.edu.cn or J. Yang; e-mail: jxy30@psu.edu
Contract grant sponsor: National Institute of Health (NIH); contract grant number: EB012575, CA182670, and HL118498
Contract grant sponsor: National Science Foundation (NSF); contract grant number: DMR1313553 and CMMI1266116
Contract grant sponsor: National Natural Sciences Foundation of China (NSFC); contract grant number: 31228007

is equally important in the success of an orthopedic tissue-engineered device.[8] Huge efforts have been devoted to the hybridization of biodegradable polymers and inorganic bioceramics to improve the mechanical properties and bioactivity of each component for orthopedic applications.[9] Although promising, many of the previous composite materials are unable to match the native bone composition, provide adequate mechanical strength, minimize inflammatory responses, promote bone regeneration, and fully integrate with the surrounding tissue.[10] For example, many of the current materials are limited by the total amount of bioceramic that can be incorporated into the composite before becoming too brittle, which ultimately limits their osteogenic potential in load bearing applications.[11] Therefore, carefully selecting the candidate polymers to composite with bioceramics at the molecular level may constitute a significant aspect in bone biomaterial design.

Designed to address the limitations of the previous materials, citrate-based hydroxyapatite (HA) composites are a new class of orthopedic biomaterial, which offer numerous advantages for orthopedic tissue engineering.[10–15] Citrate, a historically known metabolic byproduct of the Kreb's cycle, is naturally abundant in bone tissue and has been recently found to be a bound and integral part of apatite nanocrystal structure playing important roles in bone formation, stability, strength, and maintenance.[16,17] When incorporated into biomaterial design, citrate provides valuable pendant carboxyl chemistry, which improves HA calcium chelation and allows for the ability to incorporate up to 65 wt.-% HA in the composite for improved osteoconductivity and osteointegration.[18] Previous citrate-based composites are able to induce rapid mineralization *in vitro*, up regulate alkaline phosphatase (ALP) and osterix (OSX) gene expression, accelerate osteoblastic phenotype progression, and promote osteoconductivity and osteointegration *in vivo* from their ability to better replicate the native bone citrate and inorganic mineral content.[11,14,15] These recent insights have reintroduced interest into the role of citrate in bone development and have provided a new hypothesis that osteoblasts are specialized citrate producing cells providing the increased citrate levels necessary for proper bone formation.[17] Due to these multiple benefits, we believe that citrate should be considered in orthopedic biomaterial and scaffold design.

We have recently developed a clickable biodegradable citrate-based elastomer, poly (octanediol citrate)-click (POC-Click), which uses azide-alkyne cycloaddition (click chemistry) as an additional crosslinking mechanism to improve the mechanical strength of the bulk material without sacrificing valuable pendant carboxyl chemistry for HA calcium chelation.[19] In this study, biomimetic POC-Click-HA biphasic scaffolds were developed to simulate both the architectural and compositional properties of native bone tissue to provide the necessary mechanical properties, porosity, and bioceramic content. It is hypothesized that a citrate-based HA composite can provide an osteoconductive surface for bone regeneration and tissue integration, while the biphasic scaffold design can mimic the hierarchical organization of cancellous and cortical bone. A scaffold with this type of architecture can potentially provide the necessary porosity in the internal phase for tissue ingrowth with reduced porosity in the external phase to meet the immediate mechanical demands for the repair of large segmental bone defects.[4] POC-Click-HA scaffolds were fabricated and characterized for their resulting geometries, mechanical properties, and efficacy to repair 10-mm long segmental radial defects in rabbits.[20,21]

MATERIALS AND METHODS

HA [M_w: 502.32, assay >90% (as $Ca_3(PO_4)_2$); particle size: >75 μm (0.5%), 45–75 μm (1.4%), <45 μm (98.1%)] was purchased from Fluka (St Louis, MO). 1,8-octanediol (98%), citric acid (99.5%), and all remaining chemicals were purchased from Sigma-Aldrich (St Louis, MO) and used as received unless stated otherwise.

POC-Click synthesis

2,2-Bis (azidomethyl) propane-1,3-diol (diazido-diol monomer, DAzD) and propargyl 2,2-bis (hydroxyl-methyl) propionate (alkyne-diol monomer, AlD) were synthesized as described elsewhere.[22] POC-Click prepolymers with azide functionality (POC-Click-N_3) were synthesized by the copolymerization of citric acid, 1,8-octanediol, and AlD in a 1.0:0.7:0.3 molar ratio, respectively. Briefly, a mixture of citric acid and 1,8-octanediol were added to a 100 mL three-necked round bottom flask fitted with an inlet and outlet adapter. The mixture was melted under a flow of nitrogen gas by stirring at 160°C in a silicone oil bath. The temperature of the system was subsequently lowered to 120°C followed by the addition of the AlD monomer and allowed to react for 2 h to create the POC-Click-N_3 prepolymer. To remove any of the unreacted monomers and oligomers, the prepolymer was dissolved in 1,4-dioxane, and purified by drop wise precipitation in deionized water produced from a Direct-Q 5 Water Purification System (Millipore, Billerica, MA). The undissolved prepolymer was collected and lyophilized in a Freezone 6 Freeze Dryer (Labconco, Kansas City, MO) to obtain the purified pre-POC Click-N_3. POC Click prepolymers with alkyne functionality (POC-Click-Al) were synthesized as described above using citric acid, 1,8-octanediol, and DAzD in a 1.0:0.7:0.3 molar ratio, respectively.

POC-Click scaffold fabrication

Biphasic scaffold fabrication. Biphasic scaffolds consisting of similar internal phase porosities and various external phase porosities were fabricated (Fig. 1). To create the external phase, equimolar amounts of pre-POC-Click-N3 and pre-POC-Click-Al were dissolved in 1,4-dioxane and mixed with HA (65 wt.-%). Sodium chloride salt with an average size in the range of 200–400 μm was added to the mixture in various concentrations (5–50 wt %) to control the porosity of the external phase. The mixture was stirred in a Teflon dish until a homogenous viscous paste was formed. Following solvent evaporation, cylindrical shaped scaffolds were formed by inserting the viscous paste into Teflon tubes (5 × 10 mm; inner diameter × length) purchased from

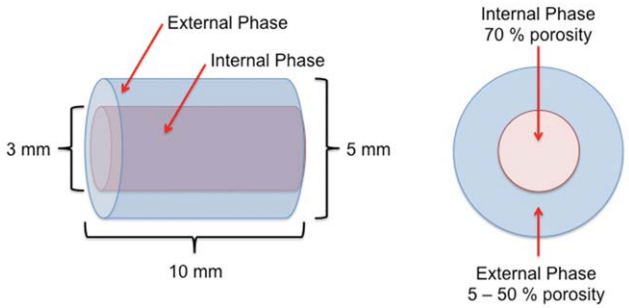

FIGURE 1. Schematic representation of the POC-Click-HA Biphasic scaffold design for long bone regeneration. Biphasic scaffolds were fabricated with similar internal phase porosities (70%) and various external phase porosities (5–50%). Biphasic scaffolds are referred to as biphasic-*X*, where *X* denotes the salt weight percentage used to create the external phase during fabrication. [Color figure can be viewed in the online issue, which is available at wileyonlinelibrary.com.]

McMaster-Carr (Aurora, OH). Finally, the scaffolds were postpolymerized in an oven maintained at 100°C for 1 day.

To create the internal phase, a 3-mm diameter hole was lathed into the center of the scaffolds, and a paste similar to the above mentioned procedure was created with a 70 wt.-% salt concentration. The resulting paste was inserted into the lumen of the external phase and allowed to dry overnight in a laminar flow hood. After solvent evaporation, the scaffolds were postpolymerized in an oven maintained at 100°C for 2 days followed by 120°C under 2 Pa vacuum for 1 day. The salt was leached out from the scaffolds by immersion in deionized water for 72 h with water changes every 12 h. Finally, the scaffolds were lyophilized to obtain the final biphasic scaffolds (5×10 mm; diameter × length). Biphasic scaffolds are referred to as biphasic-*X*, where *X* denotes the salt weight percentage used to create the external phase during fabrication. For example, biphasic-50 denotes scaffolds with 50% external phase porosity and 70% internal phase porosity.

Single-phase scaffold fabrication. To fabricate scaffolds of uniform porosity (70%), a paste similar to the inner phase fabrication was inserted into Teflon tubes (5×10 mm; inner diameter × length). Following solvent evaporation, the scaffolds were postpolymerized in an oven maintained at 100°C for 3 days followed by 120°C under 2 Pa vacuum for 1 day and processed as mentioned above.

Biphasic scaffold morphology and porosity characterization

To view the scaffold cross-sectional morphology, samples were freeze fractured using liquid nitrogen and cut using a razor. Next, the samples were sputter coated with gold and viewed under a FEI Quanta 200 environmental scanning electron microscope (SEM) (FEI, Hillsboro, OR). To characterize the scaffold geometries, three random locations were selected and a total of 30 measurements were recorded using NIH Image J analysis software (National Institute of Health, MD).

Scaffold mechanical characterization

Unconfined compression tests were performed using a 5900 series advanced electromechanical testing system (Instron, Norwood, MA). Briefly, cylindrical shaped scaffolds 5×10 mm (diameter × height) were compressed at a rate of 2 mm min^{-1} to failure. Values were converted to stress–strain and the initial modulus (MPa) was calculated from the initial gradient of the resulting curve. The peak stress (MPa) and compressive strain at break (%) were also recorded.

In vivo *scaffold evaluation*

Based on the results of *in vitro* studies, biphasic-50 scaffolds (internal phase porosity of 70% and external phase porosity of 50%) and single-phase scaffolds (uniform prosity of 70%) were chosen for the following animal study.

Animal surgery and grouping. Sixty New Zealand rabbits (Average weight, 2.1 kg) were purchased from the Laboratory Animal Center of Southern Medical University to evaluatate the potential of citrate-based scaffolds as bone substitutes to regenerate segmental bone defects. The animal experiments were carried out in compliance with a protocol approved by Southern Medical University's Institutional Animal Care and Use Committee (Guangzhou, China). The rabbits were first anesthetized with 3% sodium pentobarbital (1.5 mL/kg) by vascular injection. Prior to skin incision, the targeted left radius was shaved and disinfected. Next, a 20-mm skin incision was made, and the radial diaphysis was clearly exposed by dissecting overlying connective tissues. Using a low-speed electric saw, an *en bloc* osteoectomy was conducted to produce a 10-mm long segmental bone defect. After removing the bone segments,

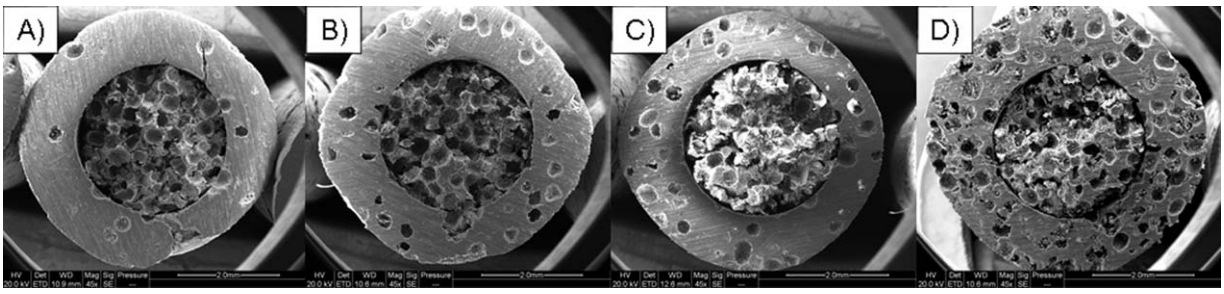

FIGURE 2. Representative SEM cross sectional images of POC-Click-HA biphasic scaffolds fabricated with a 70% internal phase porosity and (A) 5, (B) 10, (C) 24, and (D) 50% external phase porosities.

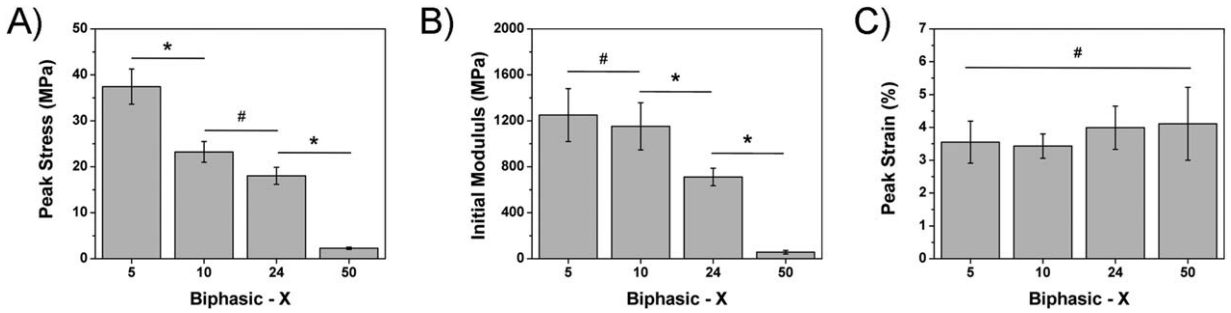

FIGURE 3. Compressive mechanical (A) peak stress, (B) initial modulus, and (C) peak strain of POC-Click-HA biphasic scaffolds fabricated with various external phase porosities (* indicates significant difference $p < 0.05$; # indicates no significant difference $p > 0.05$).

the uniform bone defects were treated with various bone grafts and randomly assigned into according groups: (1) single-phase scaffold, (2) biphasic-50 scaffolds, and (3) autologous bone grafts. As a negative control, the bone defect was left untreated. After implantation, the incision was sutured by layers, and all rabits were given penicillin for 3 days to prevent wound infection.[23] 5, 10, and 15 weeks after surgery, the rabbits were sacrificed and the radial samples were kept in 4% formalin solution for the following assessments.

Computer tomography analysis. Radial specimens from each group were subjected to computer tomography using a Micro-CT imaging system (ZKKS-MCT-Sharp-III scanner, Caskaisheng, China). Three-dimensional (3D) reconstructed images were derived with ZKKS-MicroCT 3.0 software. To quantify the bone formation in the bone defect, a rectangular area of interest was defined to cover the bone defect for quantitative evaluation. The bone mineral content (BMC) and bone mineral density (BMD) was separately measured. Data was processed with the analysis software mentioned above. To distinguish new bone from scaffolds and osteoids, the density in Micro-CT ranging from 2.5 g cm^{-3} (scaffold density) to 1.7g cm^{-3} (osteoids or native bone density) was exclusively defined as new bone formation.

Histological analysis. To conduct histological assessments, radial samples were first decalcified with ethylenediaminetetraacetic acid and embedded with paraffin. Next, the samples were cut into 4-μm thick cross-sections (at least 10 sections for each sample) and stained with hematoxylin and eosin (H&E) and Masson's Trichrome after deparaffination and dehydration.[23–25] For quantitative histological analysis, photos of bone sections were obtained under electronic microscope and the derived photos were subjected to computer-assisted histomorphometric measurements. New bone area (NBA), defined as the fraction of bone area to the whole visible field, was measured and analyzed using an automated image analysis system (FreeMaxver3.0, Zhongrui, Taiwan) equipped with a CCD camera (Kodak DCS, Atlanta, GA).

Biomechanical testing. Radial samples collected at three time points were obtained by careful dissection of surrounding soft tissues. Prior to three-point bending test, both ends of the specimens were fixed with clamps and placed on an ElectroForce 3510 Universal Material Testing Machine System (Bose, Eden Prairie, MN). Tests were conducted with an average free span of 20 mm and a deflection speed of 2 mm min^{-1}. The elastic modulus and maximal bending load was separately recorded and analyzed.[23]

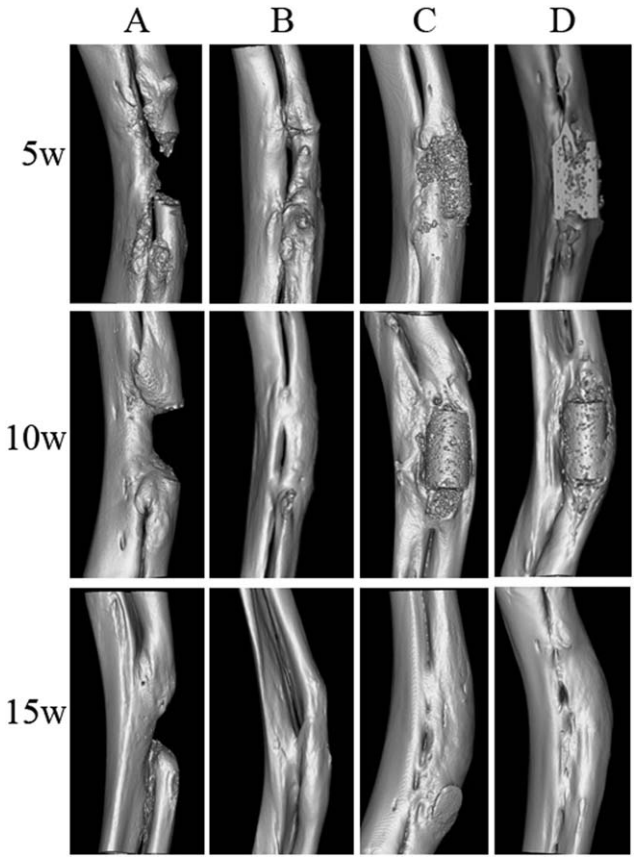

FIGURE 4. Micro-CT images of bone regeneration in radial diaphysis defects treated with (A) no bone graft (negative control), (B) autologous bone grafts, (C) POC-Click-HA single-phase scaffolds, and (D) POC-Click-HA biphasic-50 scaffolds at three predetermined time points (5, 10, and 15 weeks).

TABLE I. Rabbit Radial Bone BMC and BMD for Each Group (Mean ± SD)

	5 Weeks		10 Weeks		15 Weeks	
	BMC (mg)	BMD (mg/cm^3)	BMC (mg)	BMD (mg/cm^3)	BMC (mg)	BMD (mg/cm^3)
Empty defect	2.20 ± 0.19	574.1 ± 19.9	2.65 ± 0.21	684.3 ± 31.1	3.36 ± 0.20	743.4 ± 64.7
Single-phase	2.95 ± 0.13[a]	776.5 ± 43.1[a]	3.21 ± 0.20[a]	792.1 ± 67.2[a]	3.04 ± 0.17[a]	850.9 ± 50.9[a]
Biphasic	3.17 ± 0.16[a,b]	808.7 ± 36.6[a]	3.24 ± 0.19[a]	850.6 ± 65.1[a]	3.07 ± 0.16[a]	873.8 ± 55.3[a]
Autologous bone	3.05 ± 0.15[a]	798.7 ± 50.3[a]	3.17 ± 0.21[a]	858.7 ± 86.8[a]	3.03 ± 0.19[a]	838.2 ± 51.6[a]

[a]Significant difference from Empty defect group at the same time point ($p < 0.05$).
[b]Significant difference between Single-phase scaffold group and Biphasic-50 scaffold group at the same time point ($p < 0.05$).

Statistical analysis

Data are expressed as the mean ± standard deviation. The statistical significance between two sets of data was calculated using a two-tail Student's *t*-test. Analysis of variance (ANOVA) with Newman–Keuls multiple comparisons test *post hoc* analysis was used to determine significant differences among three or more groups. Data analysis was performed using SPSS software (SPSS, Chicago, IL). Statistical significance was noted when a $p < 0.05$ was obtained.

RESULTS

Biphasic scaffold morphology

SEM images of biphasic POC-Click-HA scaffolds fabricated with various external phase porosities are shown in Figure 2, which show the presence of two distinct scaffold architectures. Biphasic internal and external phase diameters were measured using Image J software to be 2.96 ± 0.05 mm and 5.02 ± 0.07 mm, respectively. The average pore size for all scaffolds was 338.12 ± 42.06 μm.

Biphasic scaffold mechanical properties

The fabricated scaffolds were evaluated for their compressive peak stress, initial modulus, and peak strain at break. As shown in Figure 3(A,B), a decreasing trend in peak stress and initial modulus were seen as the porosity of the external phase was increased. Compressive peak stress values significantly decreased from 37.45 ± 3.83 down to 2.26 ± 0.27 MPa for biphasic-5 and 50 scaffolds, respectively ($p < 0.05$). A similar inverse relationship was seen for the initial modulus, which shows a decrease from 1250.01 ± 230.60 down to 55.15 ± 15.83 MPa as the external phase porosity was increased from 5 to 50%. In

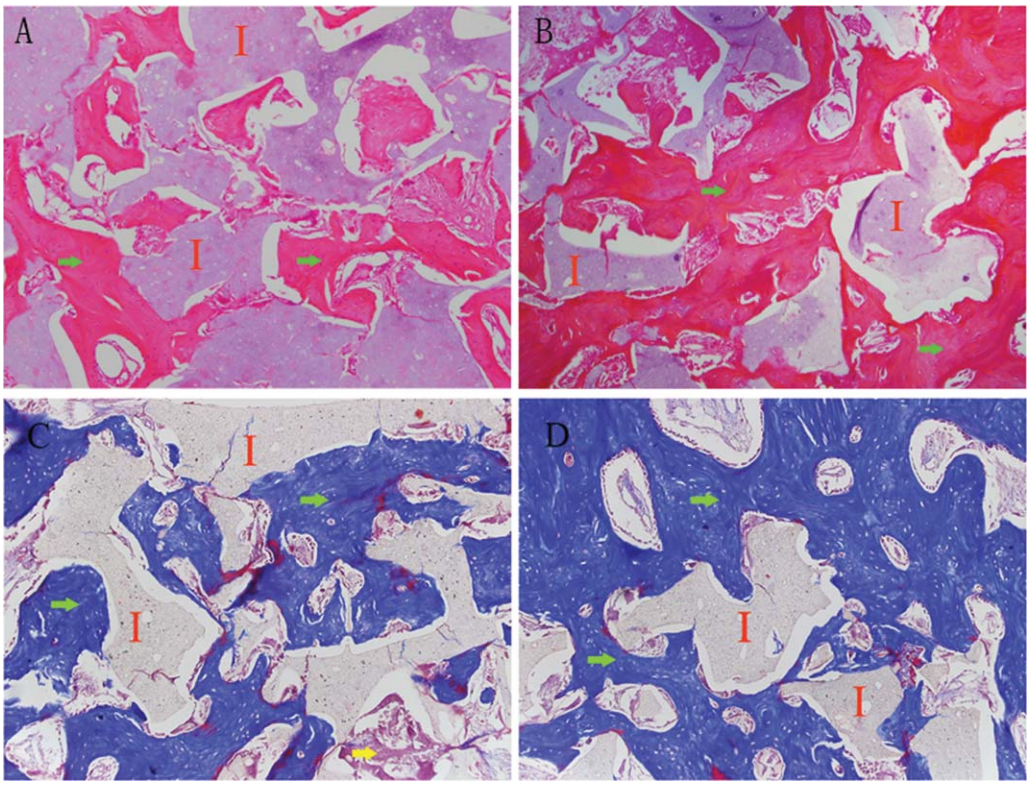

FIGURE 5. Hemotoxylin and eosin (H&E) stained and Masson's Trichrome stained sections of (A, C) POC-Click-HA single-phase scaffolds and (B, D) POC-Click-HA biphasic-50 scaffolds after 15 weeks of implantation in a 10-mm long rabbit radial defect model showing the presence of new bone formation (I: implant; Green arrow: new bone formation; Yellow arrow: fibrous tissue; magnification 200×). [Color figure can be viewed in the online issue, which is available at wileyonlinelibrary.com.]

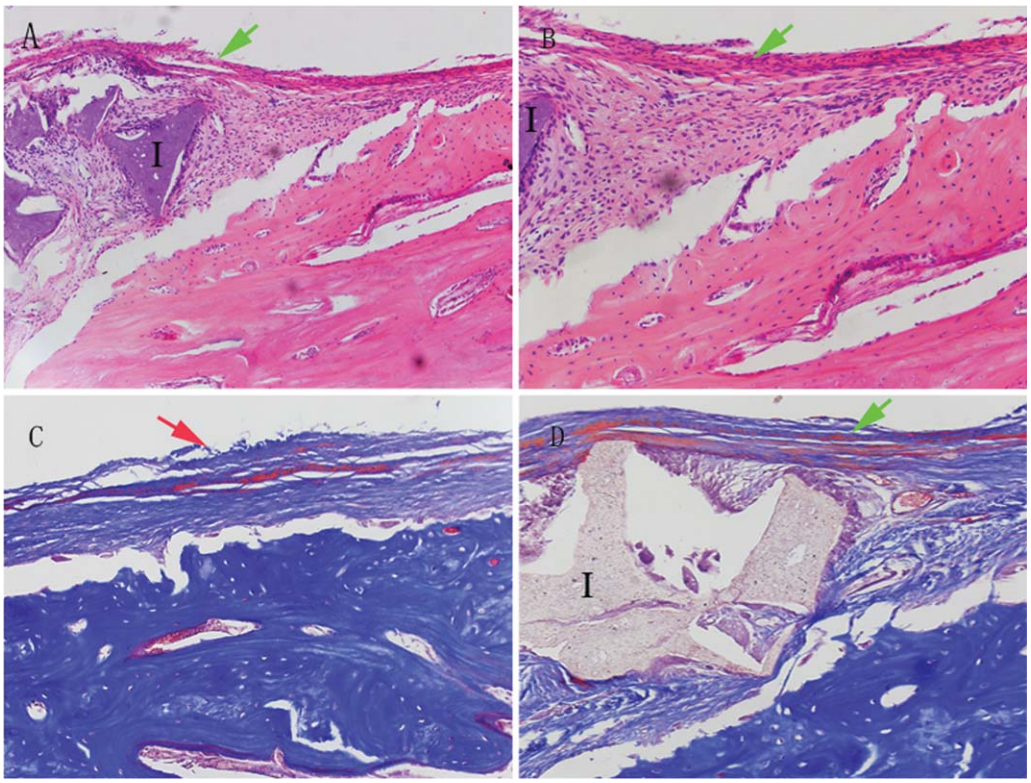

FIGURE 6. Histological assessment of periosteal remodeling bone defect sites treated with POC-Click-HA biphasic-50 scaffolds (A: H&E staining 200×, B: H&E staining 500×, and C: Masson's Trichrome Staining 500×) and in normal bone (D: Masson staining 200×) after 5 weeks of implantation. (I: POC-Click-HA Biphasic-50 implant; green arrow: periosteal remodeling; red arrow: normal periosteum). [Color figure can be viewed in the online issue, which is available at wileyonlinelibrary.com.]

contrast, Figure 3(C) shows that the compressive strain at break increased in correlation with the external phase porosity, but was not significantly different ($p > 0.05$).

Computer tomography analysis

Bone regeneration in the bone defect sites over time was recorded using 3D reconstructed micro-CT images (Fig. 4). In the negative control group, the radial segmental bone defects remained unrepaired without observable bone bridging after 15 weeks of implantation [Fig. 4(A)]. In contrast, the bone defects were regenerated and bridged to various extents in the other three groups [Fig. 4(B–D)]. For the autologous bone graft treated animals, the bone defects were bridged by new bone after 5 weeks of implantation and greatly regenerated over time. By 15 weeks, they were almost completely repaired and the medullary cavity was completely bridged. However, the diameter of the regenerated radius was smaller compared to scaffold implantation groups [Fig. 4(B)]. Fifteen weeks after implantation, the bone defects were almost completely regenerated in both scaffold groups with bridged medullary cavities [Fig. 4(C,D)]. The BMD and BMC of each group at various time points are shown in Table I. At the 5-week time point, the BMD in animals treated with biphasic scaffolds was significantly higher than those treated with single-phase scaffolds and autologous bone grafts ($p < 0.05$), but no significance was found among scaffold groups and autologous bone graft group with regard to both BMD and BMC ($p > 0.05$) in later time points.

Histological analysis

In both scaffold groups, abundant new bone formation was observed inside the scaffolds after 15 weeks of implantation (Fig. 5), and prominent periosteal remodeling around the

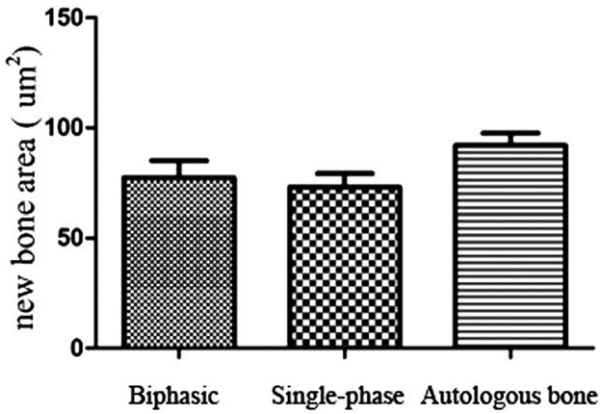

FIGURE 7. Quantitative analysis of new bone formation area (NBA) in bone defect sites treated with click-HA (POC-Click-HA) single-phase, POC-Click-HA biphasic-50, and autologous bone after 15 weeks of implanation. No statistical difference was observed among the three groups ($p > 0.05$).

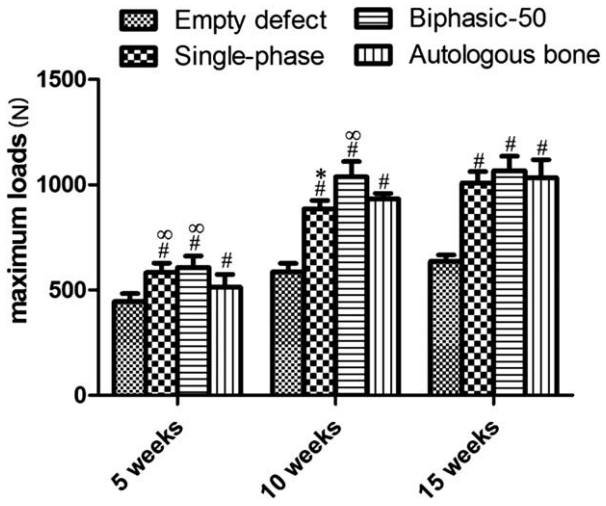

FIGURE 8. The maximum bending load of radial bones after 5, 10, and 15 weeks of surgery in which a 10 mm defect was created and treated with POC-Click-HA) single-phase, POC-Click-HA biphasic-50, autologous bone, or left empty (negative control). # indicates significant difference from empty defect group at the same time point ($p < 0.05$); * indicates significant difference between Single-phase scaffold group and Biphasic-50 scaffold group at the same time point ($p < 0.05$); ∞ indicates significant difference from autologous bone group at the same time point ($p < 0.05$).

scaffolds was observed after 5 weeks of implantation (Fig. 6). Meanwhile no obvious inflammatory response was present at the implant–bone interfaces. Compared to that of single-phase scaffolds, much less fibrous tissue was observed within the biphasic-50 scaffolds (Fig. 5). After 15 weeks of implantation, the area of new bone formation in animals treated with scaffolds was comparable to that of animals treated with autologous bone grafts (Fig. 7) ($p > 0.05$).

Biomechanical testing

The maximal bending load from three-point-bending mechanical tests are shown in Figure 8. After 5 weeks of implantation, the maximum bending loads of radii treated with single-phase and biphasic-50 scaffolds was 582.8 ± 45.1 *N* and 608.0 ± 53.6 *N*, respectively, and was significantly higher than that of autologous bone graft and negative control groups ($p < 0.05$). The difference in maximal bending load between the scaffold and autologous bone graft groups decreased over time. At the end of the 15-week study, the maximal bending load of autologous bone graft group was as high as 1066.4 ± 69.2 *N* and was comparable to that of both biphasic-50 and single phase scaffold groups, which were1034.6 ± 84.4 N and 1008.8 ± 54.2 *N*, respectively.

The elastic modulus and stiffness of rabbit radius–ulna complexes are shown in Table II. After 5 weeks of implantation, the elastic modulus and stiffness in the biphasic scaffolds were significantly higher than that in the single-phase scaffold group and autologous bone group ($p < 0.05$). After 15 weeks of implantation, there was no significant difference found between scaffold groups and autologous bone graft group ($p > 0.05$).

DISCUSSION

The repair of large segmental bone defects remains one of the most relevant challenges in reconstructive orthopedic surgery and has driven the field to look toward tissue-engineered approaches to simultaneously restore bone tissue and function. In the traditional tissue-engineering paradigm, scaffolds have served as a key component of the regenerative process by providing a 3D template for cellular organization and tissue development; however, it has recently been identified that mechanical stability following graft implantation is an equally important component in the bone healing cascade.[26,27] Unfortunately, many of the previous scaffolds designed for bone tissue engineering have focused on increasing the porosity and pore size to favor tissue ingrowth and nutrition supply. Although highly porous structures have been shown to promote cell attachment, proliferation, and differentiation, this directly results in a decrease in the biomechanical strength of the scaffold, which is a property important to the functionality of the resulting graft for load-bearing applications.[28,29] Therefore, the goal of regenerating weight-bearing bone should not only be to achieve proper anatomical morphology but also restore proper tissue function within a reasonable time frame.[30–32]

To achieve this, many researchers have looked toward nature to provide insights in the development of biologically inspired approaches, which can meet the biomimetic microarchitectural requirements for bone regeneration.[33–35] By replicating the native tissue architecture at the macroscales, microscales, and nanoscales, researchers are able to facilitate cell and extracellular matrix compartmentalization to engineer more native-like and functional tissue.[36] For example, biomimetic multiphasic and functionally graded scaffold architectures have gained recent interest from the appreciation that single-phase materials currently cannot possess the range of physiochemical properties deemed suitable for success in the biological milieu.[6] Thus, by effectively mimicking the natural multilaminated structure of cancellous and cortical bone, it was reported that HA scaffolds with multiphase porosities could induce rapid bone ingrowth into the high porosity portion and withstand physiological mechanical stress through the low porosity region after implantation.[4–7,28,37–40]

In this study, we have developed a biomimetic citrate-based biphasic scaffold to replicate the native architectural and compositional properties of native bone tissue, which can provide immediate structural support and long-term tissue regeneration for large segmental bone defects. The rationale behind the scaffold design are: (1) the use of a citrate-based material can provide a highly effective means to replicate the organic cell niche found in natural bone to improve biocompatibility and enhance bone formation; (2) citrate located in the bulk of the material provides pendant carboxyl chemistry to chelate with HA particles and allow for the incorporation of up to 65 wt.-% to match the native inorganic mineral content, which is a feature not possible with previous materials; (3) POC-Click biomaterials can be composited with HA and crosslinked through clickable

TABLE II. Three-Point-Bending Stiffness and Elastic Modulus of Rabbit Radii after 5, 10, and 15 Weeks of Surgery to Repair a 10 mm Defect Using POC-Click-HA Single Phase Scaffolds, POC-Click-HA Biphasic Scaffolds, Negative Control (Empty Defect), and Autologous Bone

	5 Weeks		10 Weeks		15 Weeks	
	Stiffness (N/m)	Elastic Modulus (MPa)	Stiffness (N/m)	Elastic Modulus (MPa)	Stiffness (N/m)	Elastic Modulus (MPa)
Empty defect	343.9 ± 24.2	93.7 ± 19.3	444.7 ± 32.7	117.9 ± 24.7	536.2 ± 31.4	143.7 ± 20.8
Single-phase	$517.5 \pm 26.4^{a,b}$	155.7 ± 25.8^{a}	735.0 ± 29.7^{a}	$195.0 \pm 29.6^{a,b}$	896.1 ± 38.2^{a}	229.9 ± 40.4^{a}
Biphasic	$697.6 \pm 24.8^{a,c}$	162.7 ± 30.3^{a}	$852.1 \pm 27.2^{a,c}$	$205.2 \pm 34.9^{a,b}$	911.5 ± 29.0^{a}	240.1 ± 32.2^{a}
Autologous bone	613.8 ± 30.1^{a}	175.4 ± 23.7^{a}	771.6 ± 39.8^{a}	252.6 ± 41.8^{a}	870.0 ± 23.0^{a}	241.3 ± 42.8^{a}

The results are expressed as the mean $\pm$ SD.
[a]Significant difference from empty defectgroup at the same time point ($p < 0.05$).
[b]significant differencefrom autologous bonegraft group at the same time point ($p < 0.05$).
[c]Significant difference between Single-phase group and Biphasic-50 group at the same time point ($p < 0.05$).

moieties to preserve valuable citrate carboxyl chemistry for HA binding resulting in strong composites; (4) A biphasic scaffold design can better simulate the bimodal distribution of highly porous cancellous bone and dense compact structure of cortical bone to provide immediate structural support following implantation; and (5) To impart porosity into the grafts, we chose to use a cost-efficient and facile solvent casting particulate leaching technique. One major advantage to this approach is that the overall dimensions, geometry, and phase porosities can be controlled using various Teflon mold and lathe drill bit dimensions to fine-tune the resulting scaffold architecture and resulting mechanical properties to meet the requirements for various anatomical locations.

SEM analysis of the POC-Click-HA biphasic scaffolds shows the clear presence of a dense external phase surrounding a porous internal phase to replicate the native cortical and cancellous bone, respectively (Fig. 2). The resulting porosities were chosen to match the respective porosities of native bone, which have been found to be 10% for cortical bone and 50–90% for cancellous bone.[41] The size of the pores was chosen to be in the range of 200–400 μm, which has previously been shown to promote bone regeneration and osteoinduction.[5] Native bone is a highly dynamic and rigid tissue. The mechanical properties of the POC-Click-HA biphasic scaffolds fabricated in this study were highly dependent on the resulting porosity of the external phase. Figure 2 shows a corresponding increase in compressive strength as the porosity of the external phase was reduced indicating that the mechanical strength of the scaffolds was primarily due to the external phase. Although the two phases do not appear to be well integrated from the SEM images, it should be noted that the respective phases were tightly bound together and did not separate after fracture during mechanical testing.

In addition to mechanical testing, the fabricated POC-Click-HA biphasic scaffolds were compared with single-phase scaffolds and autologous bone grafts to determine their ability to regenerate large segmental bone defects *in vivo* using 10-mm long rabbit radial defects. Single-phase scaffolds were included in this study to represent traditional highly porous constructs of uniform porosity. POC-Click-HA scaffolds of uniform porosity (70%) were fabricated with porosities similar to the internal phase of the biphasic scaffolds. POC-Click-HA biphasic-50 scaffolds were selected for implantation due to the well-balanced external phase porosity and scaffold strength. Histological analysis results show the presence of new bone ingrowth into both single-phase and biphasic POC-Click-HA scaffolds. Combined with micro-CT analysis, the results show that citrate-based scaffolds significantly increased BMC after 5 weeks of implantation when compared to autologous bone grafts emphasizing the importance of a porous component in the scaffold architecture, which provides the appropriate space for the migration of bone-forming cells and promotes the bone bridge connection to ultimately shorten recovery times (Table I). By the end of the study, both single-phase and biphasic scaffold architectures were able to completely repair the defect.

The remarkable bone tissue ingrowth can be attributed to the osteoinductive and osteoconductive potential of citrate-based orthopedic composites. Citrate, which is naturally abundant in skeletal tissue, has been recently implicated to play important roles in bone formation, stability, strength, and maintenance.[11,16,17,42] Surprisingly, the role of citrate has been rarely mentioned in the literature related to bone cell culture and bone development in the past 30 years including those on orthopedic biomaterials and scaffolds. The natural presence and importance of citrate in bone metabolism and physiology leads us to believe that citrate can be exploited in orthopedic biomaterial design to provide regenerative advantages not seen with previous materials. For example, our previous studies have shown that citrate-based materials have a unique ability to up regulate the *in vitro* gene expression of ALP and OSX in a pluripotent cell line, accelerate osteoblast phenotype progression, and display excellent biocompatibility and osteointegration *in vivo*.[11,14,15]

An increase in osteoinductive activity is typically correlated with an increase in HA content and porosity, but the resulting brittleness limits their use as high porosity scaffolds.[15,43] To balance the porosity needed for osteoinductive activity and the mechanical properties needed for functional restoration, biphasic scaffolds were fabricated herein.

Comprehensive biomechanical analysis of the two experimental groups revealed that the restoration of flexural strength, BMC, and modulus of the biphasic group were all significantly greater than the single-phase group, which highlights the role of a biphasic scaffold architecture in improving physiological functions during the initial periods of bone regeneration. The low porosity external phase of the biphasic scaffold design not only serves to mimic the ability of native cortical bone to withstand the biomechanical forces traversing the defect but also prevents fibrous tissue ingrowth by functioning as a barrier similar to collagen membranes. It is worthy to note that the *in vivo* results presented above on long bone regeneration were based on bare POC-Click-HA scaffolds without any additional cell seeding, supplements, or growth factors. Intensive studies have shown that a myriad of growth factors can promote bone regeneration, and whether the incorporation of a single growth factor or a cocktail of factors to potentially improve the regenerative capabilities of citrate-based bone scaffolds remains to be seen.[44,45] However, these are the first steps toward realizing the ultimate goal of this work, which is to create an off-the-shelf graft ready for immediate implantation and circumvent lengthy *in vitro* cell culture requirements for the repair of large segmental bone defects.

CONCLUSIONS

In conclusion, biomimetic citrate-based biphasic scaffolds were fabricated to replicate the native architecture of cortical and cancellous bone using a simple and cost-effective sodium chloride particulate leaching technique. Using this design, various biphasic scaffolds can be produced with tunable architectural geometries and strength. The resulting scaffolds were evaluated based on their geometry, mechanical properties, and *in vivo* performance. It is believed that architecturally and compositionally biomimetic citrate-based scaffolds can potentially serve as off-the-shelf implants to provide immediate structural support for large bone defects.

REFERENCES

1. Cancedda R, Giannoni P, Mastrogiacomo M. A tissue engineering approach to bone repair in large animal models and in clinical practice. Biomaterials 2007;28:4240–4250.
2. Horner EA, Kirkham J, Wood D, Curran S, Smith M, Thomson B, Yang XB. Long bone defect models for tissue engineering applications: Criteria for choice. Tissue Eng Part B Rev 2010;16:263–271.
3. Grayson WL, Chao PH, Marolt D, Kaplan DL, Vunjak-Novakovic G. Engineering custom-designed osteochondral tissue grafts. Trends Biotechnol 2008;26:181–189.
4. Kong L, Ao Q, Wang A, Gong K, Wang X, Lu G, Gong Y, Zhao N, Zhang X. Preparation and characterization of a multilayer biomimetic scaffold for bone tissue engineering. J Biomater Appl 2007; 22:223–239.
5. Oh SH, Park IK, Kim JM, Lee JH. In vitro and in vivo characteristics of PCL scaffolds with pore size gradient fabricated by a centrifugation method. Biomaterials 2007;28:1664–1671.
6. Lickorish D, Guan L, Davies JE. A three-phase, fully resorbable, polyester/calcium phosphate scaffold for bone tissue engineering: Evolution of scaffold design. Biomaterials 2007;28:1495–1502.
7. Soon Y-M, Shin K-H, Koh Y-H, Lee J-H, Choi W-Y, Kim H-E. Fabrication and compressive strength of porous hydroxyapatite scaffolds with a functionally graded core/shell structure. J Eur Ceram Soc 2011;31:13–18.
8. Wang H, Li Y, Zuo Y, Li J, Ma S, Cheng L. Biocompatibility and osteogenesis of biomimetic nano-hydroxyapatite/polyamide composite scaffolds for bone tissue engineering. Biomaterials 2007; 28:3338–3348.
9. Rezwan K, Chen QZ, Blaker JJ, Boccaccini AR. Biodegradable and bioactive porous polymer/inorganic composite scaffolds for bone tissue engineering. Biomaterials 2006;27:3413–3431.
10. Chung EJ, Sugimoto MJ, Ameer GA. The role of hydroxyapatite in citric acid-based nanocomposites: Surface characteristics, degradation, and osteogenicity in vitro. Acta Biomater 2011;7:4057–4063.
11. Tran RT, Wang L, Zhang C, Huang M, Tang W, Zhang C, Zhang Z, Jin D, Banik B, Brown JL, Bai X, Yang J. Synthesis and characterization of biomimetic citrate-based biodegradable composites. J Biomed Mater Res A, DOI: 10.1002/jbm.a.34928.
12. Chung EJ, Kodali P, Laskin W, Koh JL, Ameer GA. Long-term in vivo response to citric acid-based nanocomposites for orthopaedic tissue engineering. J Mater Sci Mater Med 2011;22:2131–2138.
13. Chung EJ, Qiu H, Kodali P, Yang S, Sprague SM, Hwong J, Koh J, Ameer GA. Early tissue response to citric acid-based micro- and nanocomposites. J Biomed Mater Res A 2011;96:29–37.
14. Gyawali D, Nair P, Kim HK, Yang J. Citrate-based biodegradable injectable hydrogel composites for orthopedic applications. Biomater Sci 2013;1:52–64.
15. Qiu H, Yang J, Kodali P, Koh J, Ameer GA. A citric acid-based hydroxyapatite composite for orthopedic implants. Biomaterials 2006;27:5845–5854.
16. Hu YY, Rawal A, Schmidt-Rohr K. Strongly bound citrate stabilizes the apatite nanocrystals in bone. Proc Natl Acad Sci USA 2010;107:22425–22429.
17. Costello LC, Franklin RB, Reynolds MA, Chellaiah M. The important role of osteoblasts and citrate production in bone formation: "Osteoblast Citration" as a new concept for an old relationship. Open Bone J 2012;4:27–34.
18. Jiao Y, Gyawali D, Stark JM, Akcora P, Nair P, Tran RT, Yang J. A rheological study of biodegradable injectable PEGMC/HA composite scaffolds. Soft Matter 2012;8:1499–1507.
19. Guo J, Xie Z, Tran RT, Xie D, Jin D, Bai X, Yang J. Click chemistry plays a dual role in biodegradable polymer design. Adv Mater 2014;26:1906–1911.
20. Guda T, Walker JA, Singleton BM, Hernandez JW, Son JS, Kim SG, Oh DS, Appleford MR, Ong JL, Wenke JC. Guided bone regeneration in long-bone defects with a structural hydroxyapatite graft and collagen membrane. Tissue Eng Part A 2013;19: 1879–1888.
21. Sharifi D, Khoushkerdar HR, Abedi G, Asghari A, Hesaraki S. Mechanical properties of radial bone defects treated with autogenous graft covered with hydroxyapatite in rabbit. Acta Cir Bras 2012;27:256–259.
22. Xu J, Prifti F, Song J. A Versatile monomer for preparing well-defined functional polycarbonates and poly(ester-carbonates). Macromolecules 2011;44:2660–2667.
23. Chen BL, Xie DH, Zheng ZM, Lu W, Ning CY, Li YQ, Li FB, Liao WM. Comparison of the effects of alendronate sodium and calcitonin on bone-prosthesis osseointegration in osteoporotic rats. Osteoporos Int 2011;22:265–270.
24. Chen B, Li Y, Yang X, Xie D. Comparable effects of alendronate and strontium ranelate on femur in ovariectomized rats. Calcif Tissue Int 2013;93:481–486.
25. Chen B, Li Y, Yang X, Xu H, Xie D. Zoledronic acid enhances bone-implant osseointegration more than alendronate and strontium ranelate in ovariectomized rats. Osteoporos Int 2013;24: 2115–2121.
26. Langer R, Vacanti JP. Tissue engineering. Science 1993;260:920–926.
27. Giannoudis PV, Tosounidis TI, Kanakaris NK, Kontakis G. Quantification and characterisation of endothelial injury after trauma. Injury 2007;38:1373–1381.
28. Miao X, Sun D. Graded/gradient porous biomaterials. Materials 2010;3:26–47.
29. Schumacher M, Deisinger U, Detsch R, Ziegler G. Indirect rapid prototyping of biphasic calcium phosphate scaffolds as bone

substitutes: Influence of phase composition, macroporosity and pore geometry on mechanical properties. J Mater Sci Mater Med 2010;21:3119–3127.
30. Augat P, Buhren V. Modern implant design for the osteosynthesis of osteoporotic bone fractures. Orthopade 2010;39:397–406.
31. Gansslen A. Biomechanical principles for treatment of osteoporotic fractures of the pelvis. Unfallchirurg 2010;113:272–280.
32. Yukata K, Takahashi M, Yasui N. Bone fracture and the healing mechanisms. The mechanical stress for fracture healing in view of distraction osteogenesis. Clin Calcium 2009;19:641–646.
33. da Silva JV, Martins TA, Noritomi PY. Scaffold informatics and biomimetic design: Three-dimensional medical reconstruction. Methods Mol Biol 2012;868:91–109.
34. Delcogliano M, de Caro F, Scaravella E, Ziveri G, De Biase CF, Marotta D, Marenghi P, Delcogliano A. Use of innovative biomimetic scaffold in the treatment for large osteochondral lesions of the knee. Knee Surg Sports Traumatol Arthrosc 2014;22:1260–1269.
35. Geffre CP, Margolis DS, Ruth JT, DeYoung DW, Tellis BC, Szivek JA. A novel biomimetic polymer scaffold design enhances bone ingrowth. J Biomed Mater Res A 2009;91:795–805.
36. Tran RT, Choy WM, Cao H, Qattan I, Chiao J-C, Ip WY, Yeung KW, Yang J. Fabrication and characterization of biomimetic multichanneled crosslinked-urethane-doped polyester tissue engineered nerve guides. J Biomed Mater Res A 2014;102:2793–2804.
37. Heilmann F, Standard OC, Muller FA, Hoffman M. Development of graded hydroxyapatite/CaCO(3) composite structures for bone ingrowth. J Mater Sci Mater Med 2007;18:1817–1824.
38. Pompe W, Worch H, Epple M, Friess W, Gelinsky M, Greil P, Hempel U, Scharnweber D, Schulte K. Functionally graded materials for biomedical applications. Mater Sci Eng 2003;A362:40–60.
39. Vaquette C, Fan W, Xiao Y, Hamlet S, Hutmacher DW, Ivanovski S. A biphasic scaffold design combined with cell sheet technology for simultaneous regeneration of alveolar bone/periodontal ligament complex. Biomaterials 2012;33:5560–5573.
40. Wan Y, Feng G, Shen FH, Laurencin CT, Li X. Biphasic scaffold for annulus fibrosus tissue regeneration. Biomaterials 2008;29:643–652.
41. Hao L, Harris R. Customised implant for bone replacement and growth. In: Bartolo P, Bidanda B, editors. Bio-Materials and Prototyping Applications in Medicine. New York, NY: Springer Science+Business Media, LLC; 2008. p 79–108.
42. Hartles RL. Citrate in mineralized tissues. Adv Oral Biol 1964;1:225–253.
43. Chung EJ, Sugimoto M, Koh JL, Ameer GA. Low-pressure foaming: A novel method for the fabrication of porous scaffolds for tissue engineering. Tissue Eng Part C Methods 2012;18:113–121.
44. Bose S, Tarafder S. Calcium phosphate ceramic systems in growth factor and drug delivery for bone tissue engineering: A review. Acta Biomater 2012;8:1401–1421.
45. Kempen DH, Creemers LB, Alblas J, Lu L, Verbout AJ, Yaszemski MJ, Dhert WJ. Growth factor interactions in bone regeneration. Tissue Eng Part B Rev 2010;16:551–566.